Depletion interaction between cylindrical inclusions in polymer brushes

Ji Woong Yu,[1] Daeseong Yong,[1] Bae-Yeun Ha,[2, *] and Changbong Hyeon[1, †]

[1]*Korea Institute for Advanced Study, Seoul 02455, Korea*
[2]*Department of Physics and Astronomy, University of Waterloo, Waterloo, Ontario N2L 3G1, Canada*
(Dated: November 25, 2024)

Cylindrical inclusions in mobile brushes experience apparent attraction, which arises from a tendency to minimize the depletion zone around the inclusions, thereby maximizing the overall entropy. We find that correlation blobs act as the basic units of the attraction. In tall brushes, however, the depletion zone formed above the inclusions can generate repulsion, partially offsetting the depletion attraction. Our study offers physical insights into the brush-induced depletion interaction and suggests it as a mechanism for protein cluster formation on cell surfaces.

Introduction.– Protein clusters are ubiquitous in cell membranes, and their cellular functions have been a subject of great interest [1–5]. For example, an oligomerized form of microbial rhodopsins functions as a light-driven ion-pump or ion-channel in the native membrane [6–10]. It has been shown that the glycocalyx, a layer of glycolipids and glycoproteins that densely coat the cell surface, plays vital roles in cell-cell adhesion, communication, and signaling by promoting the integrin nanocluster formation [11–14] and regulates the cancer cell progression [15]. Polymer brush-induced depletion attraction has recently been suggested as one of the key driving forces for the transmembrane protein clustering in biological membranes [16, 17], among other mechanisms, such as membrane undulation-induced thermal Casimir force [18–21], protein-protein interaction [22–25], and membrane curvature-mediated interaction [26, 27].

The attraction between inclusions in a suspension of nonabsorbing depletants characterized with purely repulsive interaction is entropic in nature, arising from an osmotic imbalance of depletants near the depletion layers [28, 29]. Although the Asakura-Oosawa (AO) theory was originally proposed for interactions between hard spheres or flat surfaces suspended in a solution of depletants in three dimensions, it can straightforwardly be extended to other geometry or polymeric systems as well as to those in two dimensions (2D) [30–33]. For extensively-studied systems of colloid-polymer mixtures [28–31, 34–45], the gyration radius of polymer (R_g) and the radius of colloidal particle (R_c) serve as the two primary length scales. Depending on their size ratio, $q = R_g/R_c$, the depletion interactions are either in the *colloid* ($q < 1$) or in the *protein limit* ($q > 1$). For our cylinder-brush system, on the other hand, where the cylinders can be deemed effectively in a semidilute solution of correlation length ξ, $q_c = \xi/D$, which replaces R_g and R_c in q with the correlation length ξ and the cylinder diameter D, becomes a relevant parameter. Together with q_c, due to the presence of another length scale set by the brush height (H) relative to the inclusion height (h), i.e., H/h, the brush-induced depletion interactions are formally categorized
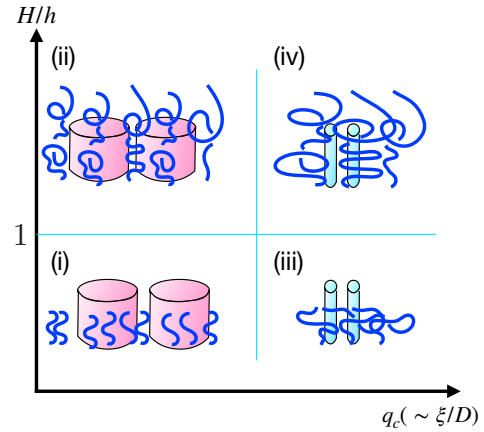

FIG. 1: Four distinct regimes of brush-induced depletion interactions between cylindrical inclusions. (i) $H/h < 1$, $q_c < 1$; (ii) $H/h > 1$, $q_c < 1$; (iii) $H/h < 1$, $q_c > 1$; (iv) $H/h > 1$, $q_c > 1$.

into four distinct regimes (Fig. 1).

Here, we first review the basics of brush polymers and revisit a quasi-2D version of the AO theory for the brush-induced depletion interaction [16]. The AO theory is employed to account for the potentials of mean force (PMFs) calculated from molecular dynamics (MD) simulations under varying brush heights and grafting densities. We not only highlight the efficacy of the blob concept [46] in quantitative understanding of depletion interactions in a brush environment, but also demonstrate that the varying brush height introduces additional complexity to the problem. Our study sheds light on membrane biophysics associated with protein nanocluster formation in glycocalyx [11–15].

Polymer brush. We consider a polymer brush where n_p polymers, each consisting of N segments, are end-grafted to a 2D surface of area A but laterally mobile on the grafting surface. When the grafting density, $\sigma = n_p/A$, is greater than that defined by the Flory radius of an isolated chain ($R_F \simeq bN^{3/5}$), i.e, $\sigma > R_F^{-2}$, the polymer chains overlap with each other and transition

from a mushroom-like configuration to a string of N/g *correlated* blobs of size $\xi(\simeq \tau^{1/5}bg^{3/5})$, forming a brush of height (H) that satisfies the Alexander-de Gennes brush scaling [47–49], $H \simeq (N/g)\,\xi \simeq Nb(\tau\sigma b^2)^{1/3}$. Here, $\tau(= (T - \Theta)/T \sim \mathcal{O}(1))$ is associated with the second virial coefficient $B_2 \sim \tau b^3$, which we set $\tau = 1$ for convenience in this paper, and σ is related to ξ as $\sigma \simeq 1/\xi^2$.

The interior of brush $(\xi < z < H)$ is effectively in the semi-dilute regime packed with correlation blobs of size ξ which changes with the polymer volume fraction $(\phi \simeq g/\xi^3)$ as $\xi \simeq b\phi^{-\gamma}$ with $\gamma = \nu/(3\nu - 1) \approx 3/4$ for $\nu = 3/5$ [46]. Thus, the osmotic pressure inside the brush is expected to follow the des Cloizeaux scaling, $\Pi/k_B T \sim 1/\xi^3 \sim \phi^{9/4}/b^3 \sim (\sigma b^2)^{3/2}$ [46, 50].

AO theory for brush-induced depletion interaction. For a brush system that contains two parallelly aligned cylindrical inclusions, mimicking signaling transmembrane receptor proteins, e.g., integrins, separated by a center-to-center distance d, the total volume accessible for brush polymers increases as the inclusions are brought together from $V(d) = V_>$ for $d > D + 2\delta_c$ to $V(d) = V_> + V_{\rm ex}(d)$ for $D \le d \le D + 2\delta_c$ with $V_> = (A - \pi D^2/2)\min(h, H) \approx A\min(h, H)$ and $V_{\rm ex}(d) > 0$. Then, according to the AO theory, the effective interaction arises from the tendency to minimize the volume of depletion zones, which in turn maximizes the accessible volume for brush polymers to explore. Thus, the AO potential is given by

$$\beta F_{\rm AO}(d; \delta_c) \simeq -n_p \left(\frac{\min(h, H)}{\xi}\right) \log\left[1 + \frac{V_{\rm ex}(d; \delta_c)}{V_>}\right]$$

$$\approx -\frac{\sigma}{\xi} V_{\rm ex}(d; \delta_c). \qquad (1)$$

Here, it is conjectured that each correlation blob contributes a free energy of $\sim \mathcal{O}(1)\, k_B T$ to the depletion interaction. Thus, $n_p \times \min(h, H)/\xi$ amounts to the number of blobs in the system. The second line of Eq. 1 is obtained from $V_{\rm ex}/V_> \ll 1$ with $\sigma = n_p/A$. Our incorporation of the blob idea [46] into the AO theory will be justified through analysis of the numerical results of brush-induced depletion interaction.

In Eq. 1, the excess volume for brush polymers is equivalent to the excess area $A_{\rm ex}(d; \delta_c)$ multiplied by the height of either brush (H) or inclusion (h), whichever is smaller, i.e., $V_{\rm ex}(d; \delta_c) = A_{\rm ex}(d; \delta_c)\min(h, H)$ with

$$A_{\rm ex}(x; \lambda_c) = \frac{D^2}{2}\left[(1 + \lambda_c)^2 \cos^{-1}\left(\frac{x}{1 + \lambda_c}\right)\right.$$

$$\left. - x^2\sqrt{\left(\frac{1 + \lambda_c}{x}\right)^2 - 1}\right] \qquad (2)$$

where we have rescaled the distance $x = d/D$ and thickness $\lambda_c = \delta_c/D$ ($1 \le x \le 1 + \lambda_c$). Thus, the AO potential
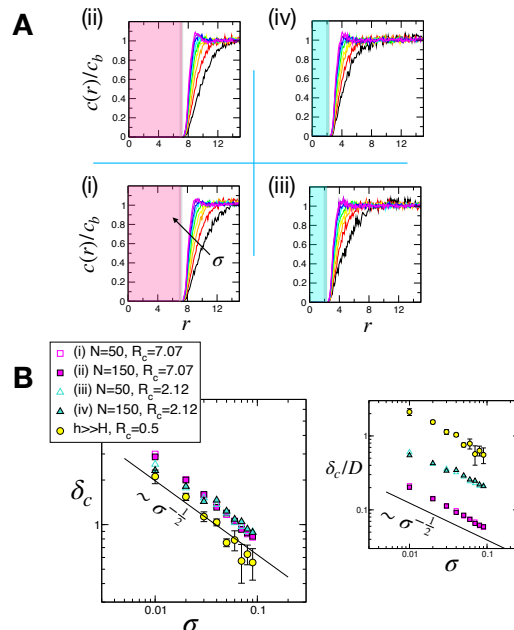

FIG. 2: (A) Monomer concentrations around a cylindrical inclusion with $R_c/b = 7.07$ (pink box) $R_c/b = 2.12$ (pale blue box) obtained from MD simulations in four distinct cases illustrated in Fig. 1. (B) Depletion layer thickness (δ_c) against grafting density (σ) for the four regimes (i–iv), and those calculated around a needle-like inclusion (yellow circles; a cylinder with $R_c/b = 0.5$ and $h \gg H$). The line of $\delta_c \sim \sigma^{-1/2}$ is depicted as a reference. (Inset) Plot of depletion layer thickness rescaled by the cylinder diameter (δ_c/D) against σ.

at x reads

$$\beta F_{\rm AO}(x) \approx -\sigma\left(\frac{\min(h, H)}{\xi}\right) A_{\rm ex}(x; \lambda_c). \qquad (3)$$

In fact, an identical expression is derived by considering the free energy gain due to the excess volume of $\min(h, H)A_{\rm ex}$ created to the semidilute solution whose osmotic pressure is given by $\beta\Pi \sim 1/\xi^3$,

$$\beta F_{\rm AO}(x) \approx -\beta\Pi \times \min(h, H)A_{\rm ex}(x; \lambda_c). \qquad (4)$$

Depletion layer thickness. To evaluate Eq. 3 or Eq. 4, it is necessary to know the depletion layer thickness (δ_c) associated with the parameter λ_c in $A_{\rm ex}(x; \lambda_c)$ (Eq.2). For colloid-polymer mixtures in a semidilute solution, it is known that $\delta_c \sim \xi$ for the colloid limit ($q = R_g/R_c \ll 1$) [30, 35], whereas for the protein limit ($q = R_g/R_c \gg 1$), δ_c is constant as $\delta_c \sim R_c$ [51, 52], independent of depletant (polymer) concentration.

For our cylinder-brush system, we calculate δ_c explicitly from the concentration profiles around a cylinder of radius $R_c(= D/2)$ (Fig. 2) through the relation [43]

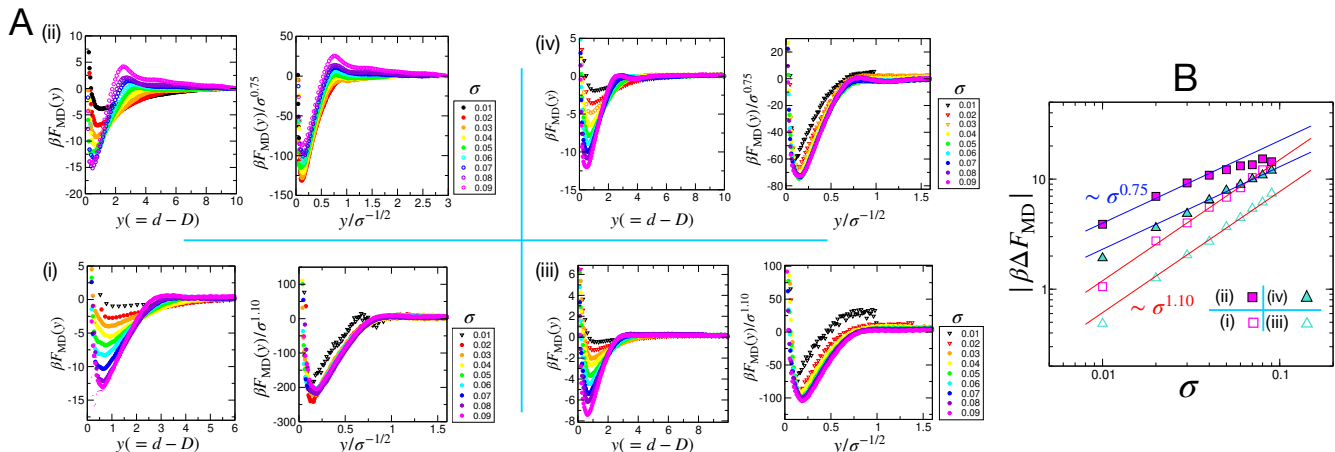$$\pi(R_c + \delta_c)^2 = \pi R_c^2 + \int_{R_c}^{\infty} 2\pi r(1 - c(r)/c_b)dr, \qquad (5)$$

FIG. 3: PMFs between cylinders with varying σ obtained from MD simulations for four distinct regimes (i)–(iv). (A) (left) PMFs versus $y = d - D$. (right) PMFs in the range of σ represented by the filled circles are collapsed onto one another when the distance and free energy are rescaled, respectively, with $\sigma^{-1/2}(= \xi)$ and σ^{α} ($\alpha = 1.10$ for $H/h < 1$ in (i) and (iii); $\alpha = 0.75$ for $H/h > 1$ in (ii) and (iv)). (B) $|\beta\Delta F_{\mathrm{MD}}|$ versus σ. The red and blue lines depict the scalings of $\sim \sigma^{1.10}$ and $\sim \sigma^{0.75}$.

where $c(r)/c_b$ is the concentration profile of monomers normalized by the bulk concentration ($c_b \equiv c(r > \xi)$) that is reached at a distance of the order of the correlation blob size [35]. For polymers grafted as in brushes, the symmetry along the brush height is broken; however, the brush height-dependence of the concentration profile around the cylinder is found insignificant. The calculations for δ_c are carried out over the range of $\sigma b^2 (= 0.01 - 0.09)$ and $D/b = 1$, $3\sqrt{2}$ and $10\sqrt{2}$, so that the parameter $q_c = \xi/D \simeq \delta_c/D \simeq (\sigma^{1/2}D)^{-1}$ encompasses the range of $q_{c,\mathrm{min}} < q_c < q_{c,\mathrm{max}}$ with $q_{c,\mathrm{min}} \simeq 0.235$ for $\sigma b^2 = 0.09$ and $D/b = 10\sqrt{2}$ and $q_{c,\mathrm{max}} \simeq 10.0$ for $\sigma b^2 = 0.01$ and $D/b = 1$ (Fig. 2).

First, the depletion layer thickness is narrow compared to the diameter of inclusion ($\delta_c/D < 1$), in effect, over the whole range of q_c being explored ($0.235 \leq q_c \leq 10.0$). Although the depletion layer thickness around the cylinder is curvature-dependent, such that smaller cylinder curvatures lead to greater δ_c's, the actual difference between δ_c's for different D is only minor (see Fig. 2). Furthermore, the difference between δ_c's for the short ($H < h$) and tall brushes ($H > h$) is not statistically significant, either (Fig. 2B).

Second, it may be tempting to associate the $q_c > 1$ limit of brush-induced depletion interaction with the *protein limit* of colloid-polymer mixtures where the depletion layer thickness is constant ($\delta_c = R_c$) [51, 52]. However, the scaling relation of $\delta_c \sim \sigma^{-1/2}$ revealed from our calculation (Fig. 2) is apparently at odds with such a notion. This signifies that the depletion layer thickness around cylindrical inclusion in brushes is dictated by the blob size ($\delta_c \sim \xi$) regardless of the size of q_c (Fig. 2) and that the correlation blob is the fundamental interaction

unit for the brush-induced depletion attraction. Note that the cylinder-brush system is distinguished from the colloid-polymer mixtures in that the axial dimension of cylinder (h) is still greater than ξ.

Analysis of PMFs from MD simulations.– The PMFs calculated from MD simulations for the four regimes illustrated in Fig. 1 are analyzed by using Eq. 3 (see Fig. 3).

For $H < h$, $\min(h, H)/\xi = H/\xi = N/g$, and Eq.2 at $x = 1$ for $\lambda_c \ll 1$ is approximated as $A_{\mathrm{ex}}(1; \lambda_c) \sim D^2 \lambda_c^{3/2} \sim D^{1/2}\delta_c^{3/2}$. From the relation of $\delta_c \sim \sigma^{-1/2}$ (Fig. 2) and the blob concept with $\nu = 0.588$, the free energy gain, $\beta F_{\mathrm{AO}}(x = 1) \equiv \beta\Delta F_{\mathrm{AO}}$ (Eq. 3), is expected to scale with σ as

$$|\beta\Delta F_{\mathrm{AO}}| \sim \sigma \left(\frac{N}{g}\right) D^{\frac{1}{2}}\delta_c^{\frac{3}{2}} \sim ND^{\frac{1}{2}}\sigma^{\frac{1}{4}+\frac{1}{2\nu}} \sim \sigma^{1.10}. \quad (6)$$

Fig. 3B shows that the dependence of stability on σ predicted by Eq.6 well accounts for the MD simulation results. In addition, upon rescaling the inclusion gap ($y = d - D$) by the blob size ($\xi \sim \sigma^{-1/2}$) and the free energy by the σ-dependent stability (Eq. 6), the rescaled free energy profiles with varying σ overlap nicely with each other (see Fig. 3A-(i) and (iii)), except for those with small σ (empty symbols in Fig. 3A) which are on the border of the brush forming regime ($\sigma R_F^2 \gtrsim 1$). On the other hand, for $H > h$, the free energy gain is characterized by a distinct exponent, 3/4, as follows:

$$|\beta\Delta F_{\mathrm{AO}}| \sim \frac{1}{\xi^3} \times hD^{\frac{1}{2}}\delta_c^{\frac{3}{2}} \sim hD^{\frac{1}{2}}\xi^{-\frac{3}{2}} \sim \sigma^{\frac{3}{4}}. \quad (7)$$

The collapsed free energy profiles upon rescaling, i.e., $(d - D) \to (d - D)/\xi$ and $\beta F_{\mathrm{MD}} \to \beta F_{\mathrm{MD}}/|\beta\Delta F_{\mathrm{AO}}|$,
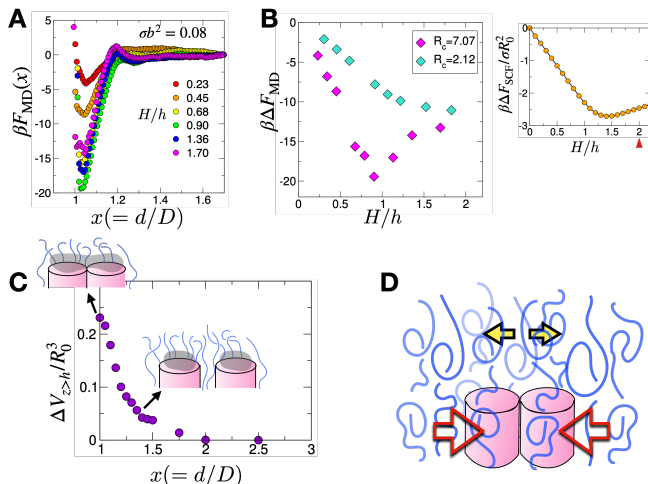
FIG. 4: (A) PMFs from MD simulations for $R_c/b = 7.07$ at $\sigma b^2 = 0.08$ with varying H/h. (B) Stabilities of two cylinders as a function of H/h for $R_c = 7.07$ and 2.12 at $\sigma b^2 = 0.08$. (Inset) Self-consistent field (SCF) calculation with the excluded volume parameter $\Lambda = 2\pi^2$. (C) Change in the volume of the depletion zone above the cylinders with increasing distance between the cylinders, $\Delta V_{z>h} = V_{z>h}(d) - V_{z>h}(\infty)$, where the volume is obtained by integrating the space whose monomer concentration is less than the 10% of bulk monomer concentration, i.e., $V_{z>h} = \int_{c(\mathbf{r}) \leq 0.1 c_b} \Theta(z - h) d\mathbf{r}$ where $\Theta(\ldots)$ is the Heaviside step function, obtained from SCF calculations at $H/h = 2$. The cartoons depict the depletion zone volume (gray) above the cylinders. (D) An illustration of depletion attraction (red arrows) and repulsion (yellow arrows) between two inclusions in tall brushes.

demonstrated in Fig.3A lend support to our analysis based on the AO theory incorporating the blob concept.

The depletion potentials and stabilities for brushes spanning from $H < h$ to $H > h$ are calculated for a fixed σ as well (Fig. 4). As predicted by the AO theory (Eq. 6), a cluster of inclusions is further stabilized with an increasing brush height H (or N) as long as $H < h$. For $H > h$, however, reduction of the stability is significant ($H/h \gtrsim 1.5$), especially for the inclusions with large $R_c(= 7.07)$ (Fig. 4B), which is no longer explicit in Eq. 7 although it correctly captures the σ-scaling.

Calculations of stability between cylinders in brushes based on self-consistent field approach, $\beta \Delta F_{\text{SCF}}/\sigma R_0^2$, the details of which will be reported elsewhere, confirms a similar trend of non-monotonic variation (the inset of Fig. 4B), validating its thermodynamic origin ruling out a kinetic effect. Our inspection of the SCF results focusing on the depletion zone (the volume inaccessible to the polymer segments, depicted in gray in Fig. 4C) *above* the cylinders ($V_{z>h}$) indicates that the reduction of the depletion zone volume is significant when two cylinders are separated apart (Fig. 4C). Just like the depletion

attraction between cylinders that results from the tendency to minimize the depletion zone around the cylinder body, repulsion arises while minimizing the excess depletion zone above the cylinders ($z > h$) surrounded by the overgrown polymer segments (the yellow arrows, Fig. 4D), and it partially offsets the depletion attraction (the red arrows, Fig. 4D) acting on the main body of the cylinders ($z < h$).

Conclusions. – The results from our analysis of brush-induced depletion interactions are recapitulated as follows. The AO theory, which relies solely on the entropy argument, i.e., the principle of minimizing the depletion zone around cylindrical objects in brushes, thereby maximizing the volume for brush polymers to explore, elucidates the origin of non-monotonic variation of depletion interaction with growing brush height. Even when the cylinder is needle-like, the cylinder height is still greater than the blob size ($D < \xi < h$). As a result, the concept of correlation blobs incorporated into the AO theory as the basic unit of depletion interactions still proves effective in quantitative characterization of the depletion layer and stability between two inclusions, making the problem of brush-induced depletion interaction unique to be differentiated from that of colloid-polymer mixtures.

Methods. – The cylinders with $D = 3\sqrt{2}b$, $10\sqrt{2}b$ and $h = 20\sqrt{2}b$ were modeled using a composite rigid body. The beads at the bottom layer ($z = 0.0$) were harmonically restrained along the z-direction with a force constant $k \simeq 10^3 \epsilon/b^2$, where ϵ is the energy scale of WCA potential described below. The brush polymers were modeled by employing the potential along the chain, $U_{\text{poly}}(r_{i,i+1}) = -(k_F R_0^2/2) \ln \left[1 - (r_{i,i+1}/R_0)^2\right] + 4\epsilon \left[(b/r_{i,i+1})^{12} - (b/r_{i,i+1})^6 + 1/4\right]$ with $k_F = 30.0\epsilon/b^2$ and $R_0 = 1.5b$. The monomers comprising the brush polymers and cylinders repel through the WCA potential $U_{\text{WCA}}(r) = 4\epsilon \left[(b/r)^{12} - (b/r)^6 + 1/4\right]$ for $0 < r < 2^{1/6}b$ and 0 otherwise. To prevent polymers from penetrating the surface at $z = 0$, the WCA potential was imposed at $z = -b$. For a given σ, n_p chains were grafted to the box that has a dimension of $L_x \times L_y$ ($L_x = L_y = \sqrt{n_p/\sigma} = 100b$) with the periodic boundary imposed along the x and y directions. Along the z direction, the shrink-wrapped boundary condition was used. Two distinct sizes of brush polymer, $N = 50$ and 150, were employed to simulate the regimes of (i), (iii) ($H < h$) and (ii), (iv) ($H > h$) in Fig. 1, respectively.

The Large-scale Atomic/Molecular Massively Parallel Simulator (LAMMPS) [53] was used for the MD simulations. To calculate the PMF between the cylinders, the umbrella sampling was performed at the temperature $T = 1.0 \; \epsilon/k_B$, with k_B the Boltzmann constant. At each sampling point, the system was first relaxed for

$10^3\tau$, followed by a production run for $10^5\tau$ under a bias potential, $U_\mathrm{b}\left(d;d_j\right) = k_\mathrm{b}\left(d - d_j\right)^2/2$, with $k_\mathrm{b} = 200.0$ ϵ/b^2 and $d_j = D + 10b - jb/4$ $(j = 1, ..., 42)$. The unbiased free energy profile was reconstructed through the weighted histogram analysis method (WHAM) [54].

* byha@uwaterloo.ca
† hyeoncb@kias.re.kr

[1] M. Aivaliotis, P. Samolis, E. Neofotistou, H. Remigy, A. K. Rizos, and G. Tsiotis, Biochimica et Biophysica Acta (BBA)-Biomembranes **1615**, 69 (2003).
[2] T. Lang and S. O. Rizzoli, Physiology **25**, 116 (2010).
[3] F. Baumgart, A. M. Arnold, K. Leskovar, K. Staszek, M. Fölser, J. Weghuber, H. Stockinger, and G. J. Schütz, Nat. Methods **13**, 661 (2016).
[4] T. Lukeš, D. Glatzová, Z. Kvíčalová, F. Levet, A. Benda, S. Letschert, M. Sauer, T. Brdička, T. Lasser, and M. Cebecauer, Nat. Commun. **8**, 1 (2017).
[5] J. J. Sieber, K. I. Willig, R. Heintzmann, S. W. Hell, and T. Lang, Biophys. J. **90**, 2843 (2006).
[6] R. Henderson and P. N. T. Unwin, Nature **257**, 28 (1975).
[7] A. L. Klyszejko, S. Shastri, S. A. Mari, H. Grubmüller, D. J. Muller, and C. Glaubitz, J. Mol. Biol. **376**, 35 (2008).
[8] K. T. Sapra, H. Besir, D. Oesterhelt, and D. J. Muller, J. Mol. Biol. **355**, 640 (2006).
[9] S. Hussain, M. Kinnebrew, N. S. Schonenbach, E. Aye, and S. Han, J. Mol. Biol. **427**, 1278 (2015).
[10] T. Morizumi, W.-L. Ou, N. Van Eps, K. Inoue, H. Kandori, L. S. Brown, and O. P. Ernst, Scientific Reports **9**, 11283 (2019).
[11] G. S. Offeddu, C. Hajal, C. R. Foley, Z. Wan, L. Ibrahim, M. F. Coughlin, and R. D. Kamm, Commun. Biol. **4**, 255 (2021).
[12] N. Kanyo, K. D. Kovacs, A. Saftics, I. Szekacs, B. Peter, A. R. Santa-Maria, F. R. Walter, A. Dér, M. A. Deli, and R. Horvath, Scientific reports **10**, 22422 (2020).
[13] A. Buffone Jr and V. M. Weaver, J. Cell. Biol. **219**, e201910070 (2019).
[14] C. R. Shurer, J. C.-H. Kuo, L. M. Roberts, J. G. Gandhi, M. J. Colville, T. A. Enoki, H. Pan, J. Su, J. M. Noble, M. J. Hollander, et al., Cell **177**, 1757 (2019).
[15] M. J. Paszek, C. C. DuFort, O. Rossier, R. Bainer, J. K. Mouw, K. Godula, J. E. Hudak, J. N. Lakins, A. C. Wijekoon, L. Cassereau, et al., Nature **511**, 319 (2014).
[16] A. M. Tom, W. K. Kim, and C. Hyeon, J. Chem. Phys.

[17] R. K. Spencer and B.-Y. Ha, Macromolecules **54**, 1304–1313 (2021).
[18] M. Goulian, R. Bruinsma, and P. A. Pincus, Europhys. Lett. **22**, 145 (1993).
[19] J.-M. Park and T. Lubensky, J. Phys. I **6**, 1217 (1996).
[20] B. B. Machta, S. L. Veatch, and J. P. Sethna, Phys. Rev. Lett. **109**, 138101 (2012).
[21] B. Spreng, H. Berthoumieux, A. Lambrecht, A.-F. Bitbol, P. M. Neto, and S. Reynaud, New J. Phys. **26**, 013009 (2024).
[22] N. Ben-Tal and B. Honig, Biophys. J. **71**, 3046 (1996).
[23] U. Schmidt, G. Guigas, and M. Weiss, Phys. Rev. Lett. **101**, 128104 (2008).
[24] B. West, F. L. Brown, and F. Schmid, Biophys. J. **96**, 101 (2009).
[25] D. Milovanovic, A. Honigmann, S. Koike, F. Göttfert, G. Pähler, M. Junius, S. Müllar, U. Diederichsen, A. Janshoff, H. Grubmüller, et al., Nat. Commun. **6**, 1 (2015).
[26] B. J. Reynwar, G. Illya, V. A. Harmandaris, M. M. Müller, K. Kremer, and M. Deserno, Nature **447**, 461 (2007).
[27] H. T. McMahon and J. L. Gallop, Nature **438**, 590 (2005).
[28] S. Asakura and F. Oosawa, J. Chem. Phys. **22**, 1255 (1954).
[29] S. Asakura and F. Oosawa, J. Polym. Sci. **33**, 183 (1958).
[30] H. N. W. Lekkerkerker, R. Tuinier, and M. Vis, *Colloids and the depletion interaction* (Springer Nature, 2024).
[31] K. Miyazaki, K. Schweizer, D. Thirumalai, R. Tuinier, and E. Zaccarelli, J. Chem. Phys. **156** (2022).
[32] H. Kang, P. A. Pincus, C. Hyeon, and D. Thirumalai, Phys. Rev. Lett. **114**, 068303 (2015).
[33] H. Kang, N. M. Toan, C. Hyeon, and D. Thirumalai, J. Am. Chem. Soc. **137**, 10970 (2015).
[34] A. Vrij, Pure Appl. Chem. **48**, 471 (1976).
[35] J. Joanny, L. Leibler, and P. G. de Gennes, J. Polym. Sci., Part B: Polym. Phys. **17**, 1073 (1979).
[36] H. De Hek and A. Vrij, J. Colloid. interface Sci. **84**, 409 (1981).
[37] M. R. Shaw and D. Thirumalai, Phys. Rev. A **44**, R4797 (1991).
[38] Y. Mao, M. Cates, and H. N. W. Lekkerkerker, Physica A: Statistical Mechanics and its Applications **222**, 10 (1995).
[39] Y. Mao, M. Cates, and H. N. W. Lekkerkerker, Phys. Rev. Lett. **75**, 4548 (1995).
[40] T. Biben, P. Bladon, and D. Frenkel, J. Phys.: Condensed Matter **8**, 10799 (1996).
[41] Y. Mao, M. Cates, and H. N. W. Lekkerkerker, J. Chem. Phys. **106**, 3721 (1997).
[42] A. Hanke, E. Eisenriegler, and S. Dietrich, Phys. Rev. E. **59**, 6853 (1999).
[43] D. Aarts, R. Tuinier, and H. N. W. Lekkerkerker, J. Phys. : Condensed Matter **14**, 7551 (2002).
[44] D. Marrenduzzo, K. Finan, and P. R. Cook, J. Cell. Biol. **175**, 681 (2006).
[45] K. Binder, P. Virnau, and A. Statt, J. Chem. Phys. **141**, 559 (2014).
[46] P. G. de Gennes, *Scaling Concepts in Polymer Physics*

154 (2021).

(Cornell University Press, Ithaca and London, 1979).

[47] S. Alexander, J. Phys. **38**, 983 (1977).

[48] P. G. de Gennes, Macromolecules **13**, 1069 (1980).

[49] P. G. de Gennes, Adv. Colloid Interface Sci. **27**, 189 (1987).

[50] P. L. Hansen, J. A. Cohen, R. Podgornik, and V. A. Parsegian, Biophys. J. **84**, 350 (2003).

[51] T. Odijk, Macromolecules **29**, 1842 (1996).

[52] R. P. Sear, Phys. Rev. E **56**, 4463 (1997).

[53] A. P. Thompson, H. M. Aktulga, R. Berger, D. S. Bolintineanu, W. M. Brown, P. S. Crozier, P. J. In't Veld, A. Kohlmeyer, S. G. Moore, T. D. Nguyen, et al., Computer Physics Communications **271**, 108171 (2022).

[54] S. Kumar, D. Bouzida, R. H. Swendsen, P. A. Kollman, and J. M. Rosenberg, J. Comp. Chem. **13**, 1011 (1992).